Hindawi Publishing Corporation
Journal of Biomedicine and Biotechnology
Volume 2008, Article ID 841312, 6 pages
doi:10.1155/2008/841312

Research Article

Structure-Based Inhibitors Exhibit Differential Activities against *Helicobacter pylori* and *Escherichia coli* Undecaprenyl Pyrophosphate Synthases

Chih-Jung Kuo,[1,2] Rey-Ting Guo,[1,2] I-Lin Lu,[3] Hun-Ge Liu,[4] Su-Ying Wu,[3] Tzu-Ping Ko,[4] Andrew H.-J. Wang,[1,2,4] and Po-Huang Liang[1,2,4]

[1] *Taiwan International Graduate Program, Academia Sinica, Taipei 115, Taiwan*
[2] *Institute of Biochemical Sciences, National Taiwan University, Taipei 106, Taiwan*
[3] *Division of Biotechnology and Pharmaceutical Research, National Health Research Institutes, Chu-Nan, Miaw-Li 350, Taiwan*
[4] *Institute of Biological Chemistry, Academia Sinica, Taipei 11529, Taiwan*

Correspondence should be addressed to Po-Huang Liang, phliang@gate.sinica.edu.tw

Received 21 September 2007; Accepted 27 December 2007

Recommended by Daniel Howard

Helicobacter Pylori colonizes the human gastric epithelium and causes diseases such as gastritis, peptic ulcers, and stomach cancer. Undecaprenyl pyrophosphate synthase (UPPS), which catalyzes consecutive condensation reactions of farnesyl pyrophosphate with eight isopentenyl pyrophosphate to form lipid carrier for bacterial peptidoglycan biosynthesis, represents a potential target for developing new antibiotics. In this study, we solved the crystal structure of *H. pylori* UPPS and performed virtual screening of inhibitors from a library of 58,635 compounds. Two hits were found to exhibit differential activities against *Helicobacter Pylori* and *Escherichia coli* UPPS, giving the possibility of developing antibiotics specially targeting pathogenic *H. pylori* without killing the intestinal *E. coli*.

1. INTRODUCTION

Undecaprenyl pyrophosphate synthase (UPPS) catalyzes consecutive condensation reactions of farnesyl pyrophosphate (FPP) with eight molecules of isopentenyl pyrophosphate (IPP) to form C_{55} undecaprenyl pyrophosphate (UPP), which acts as a lipid carrier to mediate bacterial peptidoglycan biosynthesis [1, 2]. This enzyme belongs to a group of *cis*-prenyltransferases which catalyze *cis*-double bonds during IPP condensation reactions [3, 4]. UPPS was first cloned from *Micrococcus luteus* and *Escherichia coli*, and their amino acid sequences were found conserved among the *cis*-prenyltransferases, but totally different from those of the *trans*-prenyltransferases [5–7], implying different catalytic mechanism [8, 9].

Helicobacter Pylori is a pathogen which causes chronic inflammation in the stomach [10]. The infection may evolve to peptic ulcerations and gastric neoplasias. Due to its unusual ability to survive in stomach under the low pH condition via proton pumps, *H. Pylori* infection becomes wide spreading and accounts for the increased cases of stomach carcinogenesis [11]. Antibiotics, such as proton pump inhibitors (PPI), amoxicillin, and clarithromycin, are used to treat the infected patients. When failed, empirical quadruple therapy (PPI-bismuch-tetracyclin-metronidazole) is then used as the second-line therapy [12]. Since UPPS is essential for bacterial survival, it could possibly serve as a target for new antibiotics. Even though the complex structures of *E. coli* UPPS with the FPP substrate or with its analogue (farnesyl thiopyrophosphate, FsPP) and IPP have been obtained [9, 13], no UPPS structure-derived inhibitors have been reported so far. As shown in this study, we solved the crystal structures of *H. pylori* UPPS and performed structure-based inhibitor discovery. Two hits were discovered through computer virtual screening from 58,635 compounds, which exhibited different level of inhibition against *E. coli* and *H. pylori* UPPS.

2. MATERIALS AND METHODS

2.1. Overexpression of H. pylori UPPS

The gene encoding UPPS from the *H. pylori* (ATCC43504) genomic DNA was amplified by using polymerase chain

reaction (PCR). The forward primer 5′-GGTATTGAGGGTCGCTTGGATAGCACTCTCAAA-3′ and reverse primer 5′-AGAGGAGAGTTAGAGCCCTAGCATTTTAATTCCCC-3′ were utilized in the PCR. The PCR product was purified from 0.8% agarose gel electrophoresis. The DNA product was ligated with pET-32Xa/LIC vector and transformed into *E. coli* BL21 (DE3) for protein expression as previously described for expressing *E. coli* UPPS [14].

The C234A mutant was prepared by using QuikChange Site-Directed Mutagenesis Kit in conjunction with the wild-type gene template in the pET32Xa/Lic vector. The mutagenic forward primer was 5′-CGCAAATTCGGGGAATTAAAA GCC TAGTGAGGCTCTAACTCT-3′. The procedure of mutagenesis utilized a supercoiled double-stranded DNA (dsDNA) vector with an insert of interest and two synthetic forward and backward primers containing the desired mutation. The mutation was confirmed by sequencing the entire UPPS mutant gene of the plasmid obtained from overnight culture. The correct construct was subsequently transformed to *E. coli* BL21(DE3) for protein expression. The procedure for protein purification followed our reported protocol [15]. Each purified mutant UPPS was verified by mass spectroscopic analysis and its purity (>95%) was checked by SDS-PAGE.

2.2. Crystallization and data collection

H. pylori C234A UPPS mutant was crystallized using the hanging drop method from Hampton Research (Laguna Niguel, Calif, USA) by mixing 2 μL of the UPPS solution (10 mg/mL in 25 mM Tris, 150 mM NaCl, pH 8.0) with 2 μL of the mother liquor (0.15 M KSCN, 15% PEG600, and 2% PEG5KMME), and equilibrating with 500 μL of the mother liquor. Within 4 days, crystals grew to dimensions of about $0.5 \times 0.5 \times 0.2$ mm, and then the crystals were soaked with a cryoprotectant solution of 0.2 M KSCN, 30% PEG600, and 5% PEG5KMME for 1 day. The structure of the C234A *H. pylori* UPPS in complex with FsPP was obtained by soaking the crystals with cryoprotectant solution of 2.5 mM $MgCl_2$, 2.5 mM IPP, 2.5 mM FsPP, 0.15 M KSCN, 15% PEG600, and 2% PEG5KMME. However, only the pyrophosphate of FsPP was found in the complex structure. The X-ray diffraction datasets for the structures of the C234A UPPS mutant and the complex with FsPP were collected to 1.88 Å and 2.5 Å resolution, respectively. Data for the C234A UPPS crystals were collected at beam line BL17B2 of the National Synchrotron Radiation Research Center (NSRRC, Hsinchu, Taiwan). Data for the C234A UPPS complexed with FsPP were collected in house using a Rigaku MicroMax002 X-ray generator equipped with an *R*-Axis IV++ image plate detector. The diffraction data were processed using the programs of HKL and HKL2000 [16]. Statistics for the dataset are listed in Table 1. Prior to use in structural refinements, 5% randomly selected reflections were set aside for calculating R_{free} as a monitor [17].

2.3. Structure determination and refinement

The crystal structure of C234A UPPS was determined by molecular replacement method using the *Crystallography* & *NMR System* (CNS) program [18]. The orthorhombic crystal contained one UPPS dimer in an asymmetric unit. The models of PDB 1V7U (*E. coli* UPPS structure bound with FPP, chain A) [13] were used as search model to yield a good resolution for the *H. pylori* UPPS. The space group was determined as $P2_12_12_1$. With all solvent and cofactor molecules removed, the model yielded an initial *R*-value of 0.50 using all positive reflections at 1.88 Å resolution upon rigid-body refinement.

The 2Fo-Fc difference Fourier map showed clear electron densities for most amino acid residues. The residues of catalytic loop of 58–67 in chain A, 56–71 and 150–158 in chain B were disordered. Subsequent refinement with incorporation of 581 water molecules according to 1.0 σ map level yielded *R* and R_{free} values of 0.193 and 0.240, respectively, at 1.88 Å resolution. By employing similar procedures, the C234A *H. pylori* UPPS and the FsPP-complexed structures were refined with the addition of cofactor and solvent

Table 1: Data collection and refinement statistics for the orthorhombic *H. pylori* UPPS crystals of the apoenyzme and the complex with thiopyrophosphate. C234A mutation was included to prevent intramolecular disulfide bond formation.

	H. pylori UPPS	*H. pylori* UPPS + PPi
Data collection		
Space group	$P2_12_12_1$	
Resolution (Å)[a]	25 to 1.88 (1.95 to 1.88)	50 to 2.5 (2.59 to 2.5)
Unit cell dimensions		
a, b, c (Å)	49.63, 58.91, 153.43	
No. of reflections		
Observed	201171 (18692)	137910 (12888)
Unique	35917 (3338)	15618 (1432)
Completeness (%)	95.4 (90.3)	96.0 (91.2)
R_{merge} (%)	5.5 (43.3)	5.9 (15.9)
$I/\sigma(I)$	30.7 (4.1)	42.3 (5.2)
Refinement		
No. of reflections[b]	34629 (3038)	15084 (1330)
R_{work} (%)	19.34 (22.91)	21.44 (30.24)
R_{free} (%)	24.00 (30.02)	29.33 (37.43)
Geometry deviations		
Bond lengths (Å)	0.0193	0.0061
Bond angles (°)	1.817	1.157
No. of all non-H atoms	3463	3449
No. of water molecules	581	134
Mean B-values (Å^2)	39.54	49.49
Ramachandran plot (%)		
Most favored	92.1	92.3
Additionally allowed	7.9	7.7

[a]Values in the parentheses are for the highest resolution shells.
[b]All positive reflections are used in the refinements.

molecules. All manual modifications of the models were performed on an SGI Fuel computer using the program O [19]. Computational refinements, which included maximal likelihood and simulated-annealing protocols, were carried out using CNS. The programs MolScript [20], and Raster3D [21] were used in producing figures.

2.4. Computer screening to identify the inhibitors

The X-ray structure of *H. pylori* UPPS reported here and the complex structure of *E. coli* UPPS (PDB code 1V7U) were chosen as the templates in the virtual screening. The program GOLD V2.1 was used to screen Maybridge database, a commercially available compound database obtained from Maybridge Chemical Company (Tintagel, Cornwall, England). The binding pocket for the docking study was defined as a 15 Å radius sphere centered on the active site Asp13 of *H. pylori* UPPS or Asp26 of *E. coli* UPPS. The scoring function, GoldScore, implemented in GOLD was used to rank the docking positions of the compounds. 26 compounds with the highest score ranked by GoldScore were selected for inhibition assays.

2.5. IC_{50} determination

The IC_{50} values of the two hits were measured in a buffer of 100 mM Hepes (pH 7.5), 50 mM KCl, 0.5 mM $MgCl_2$, and 0.1% Triton X-100, containing 0.05 μM of *E. coli* or *H. pylori* UPPS. The concentrations of inhibitors used were ranged from 0 to 500 μM. To obtain the IC_{50}, the does-response curves were fitted with the equation, $A(I) = A(0)\times\{1-[I/(I+IC_{50})]\}$, where A(I) is the enzyme activity with inhibitor concentration I, A(0) is enzyme activity without inhibitor, and I is the inhibitor concentration.

3. RESULTS

3.1. 3D structures of H. pylori UPPS

To develop structure-based inhibitors, the crystal structures of *H. pylori* UPPS were solved in this study. One is the structure of *H. pylori* UPPS containing C234A mutation to prevent intra-molecular disulfide bond formed during the long period of crystallization process (Figure 1(a)), and the other is the structure of C234A complexed with FsPP, but only the pyrophosphate portion is visible (Figure 1(b)). The C234A mutant has unchanged kinetic property compared with the wild type (k_{cat}, FPP K_m and IPP K_m of C234A were $0.20\pm0.08\ s^{-1}$, $0.15\pm0.04\ \mu$M and $9.6\pm0.2\ \mu$M, almost equal to $0.22\pm0.05\ s^{-1}$, $0.11\pm0.02\ \mu$M and $9.2\pm0.1\ \mu$M for the wild type, resp.). The overall structure of *H. pylori* UPPS was similar to that of *E. coli* UPPS [22]. The protein is a dimer and each subunit contains a catalytic domain and a pairing domain. Two subunits are tightly associated through the central β-sheet and a pair of long α-helices (α5 and α6). However, *H. pylori* UPPS has a 1.5-turn shorter α5 helix in the dimer interface. This may weaken the dimer formation for *H. pylori* UPPS. The catalytic domain is composed of six β-strands and four β-helices and the central tunnel-shaped active site is surrounded by 2 α-helices (α2 and α3) and 4 β-strands (βA-βB-βD-βC) (Figure 1(a)).

At the bottom of the tunnel, a large amino acid F124 occupies a similar position to that of L137 at the bottom of *E. coli* UPPS tunnel, which is a key residue to shield the final product and determine its chain length [22]. At the top of this tunnel, several amino acids including D13, R17, R26, H30, F57, S58, R180, and E184 are located in the substrate binding site (Figure 1(b)). The position of the pyrophosphate (shown in black sticks in Figure 1(b)) of FsPP in the complex is almost identical to that of the FPP pyrophosphate in the *E. coli* UPPS active site [13].

The positions of the α3 helix in the two subunits of *H. pylori* UPPS are slightly different (Figure 1(a)), resembling the open and closed forms of *E. coli* UPPS [22]. *H. pylori* UPPS A-chain strongly resembles the Triton-bound open form of *E. coli* UPPS [23], with root mean square deviation (r.m.s.d) of 0.78 Å for 200 match pairs of α-carbon atoms. Compare to the closed-form structure of *E. coli* UPPS with FsPP and IPP bound [9], the *H. pylori* UPPS B-chain is with the r.m.s.d. of 1.08 Å for 191 match pairs of α-carbon atoms. This suggests a conformational change in the *H. pylori* UPPS reaction.

3.2. Virtual screening of the H. pylori UPPS inhibitors

Based on the structures, computer virtual screening was carried out to search for selective inhibitors of *E. coli* and *H. pylori* UPPS. The screening procedure is summarized in Figure 2. The crystal structure of *E. coli* UPPS bound with FPP (1V7U) was used as a template first for the virtual screening since the electron density of a small loop responsible for conformational change near the active site is not visible in *H. pylori* UPPS, which might confound the virtual screening result. A compound database containing 58,635 compounds available from Maybridge Chemical Company were screened using the program GOLD V2.1. Each compound in the database was docked into the active site of *E. coli* UPPS, defined as 15 Å radius sphere around Asp26, an essential residue responsible to coordinate with the catalytic Mg^{2+}. The docked molecules were then ranked by the GoldScore fitness function, according to the sum of H-bond energy, van der Waals energy, internal ligand van der Waals and internal torsional strain energy. The top 26 compounds ranked by GoldScore were then purchased and experimentally evaluated for their ability to inhibit *H. pylori* and *E. coli* UPPS.

3.3. Inhibition against E. coli and H. pylori UPPS

Of these 26 compounds, 2 compounds numbered BTB06061 and HTS04781, were found inhibitory to *H. pylori* UPPS almost equally with IC_{50} values of 350 μM and 362 μM, respectively (Figure 3). The IC_{50} values of these two compounds against the C234A and wild-type enzyme were almost equal. As revealed by the predicted models shown in Figures 3(a) and 3(b), two inhibitors are likely bound to *H. pylori* UPPS with a similar orientation to that of the substrate FPP. The sulfur atom in the thiazole ring of BTB06061 may form H-bonds with Asn15 and His30 while the SO_2 group is hydrogen bound with Met12. In addition,

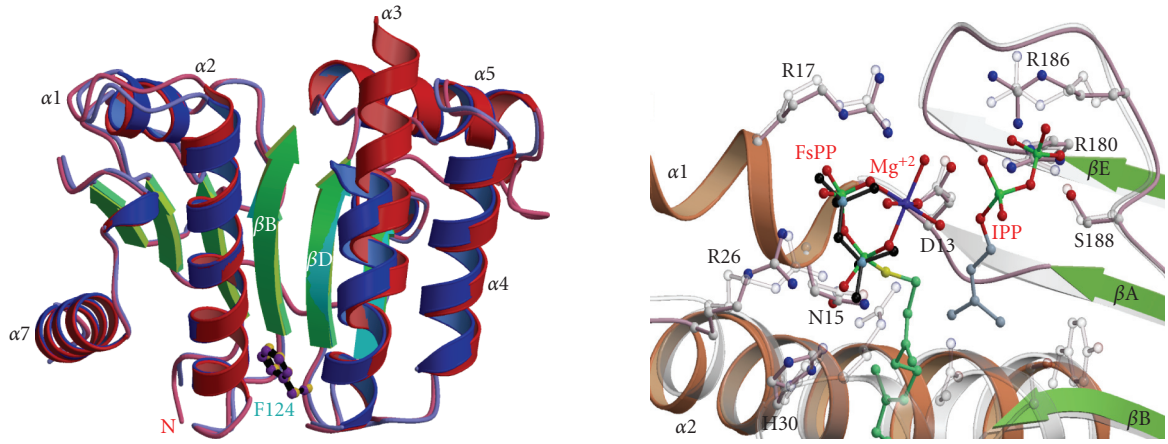

Figure 1: *Crystal structures of H. pylori UPPS.* (a) Two subunits of the apoenzyme are superimposed. The most obvious disposition occurs in $\alpha 3$ helix which adopts an open form and a closed form in subunit A and B, respectively. At the top of the tunnel-shaped crevice surrounded by 2α-helices and 4β-strands is the substrate-binding site. Phe124 located at the bottom of the *H. pylori* UPPS tunnel adopts a similar position to that of Leu137 in *E. coli* UPPS, essential for determining product chain length. (b) Superimposition of active site structures of *H. pylori* UPPS with FsPP and *E. coli* UPPS with FsPP, Mg^{2+}, and IPP [9]. The active site residues in *H. pylori* UPPS are shown in pink and those in *E. coli* UPPS in white for carbon-carbon bonds in ball-and-stick model. The thiopyrophosphate (visible in crystal structure) is shown in black, the nitrogen atoms and Mg^{2+} ion are shown in blue, and oxygen atoms are shown in red. Asp13 in *H. pylori* UPPS occupies a similar position to that of Asp26 in *E. coli* UPPS to coordinate with an Mg^{2+} for binding with the pyrophosphate leaving group of FPP.

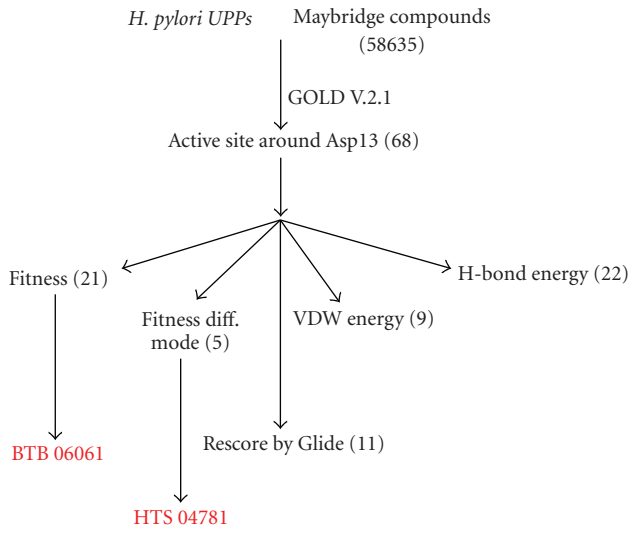

Figure 2: *The flow chart for computer screening of H. pylori UPPS inhibitors.* The active zone for screening was focused on Asp13, an important amino acid residue for coordinating with catalytic Mg^{2+}. In parentheses are the numbers of compounds. BTB06061 and HTS04781 are the final hits.

the aromatic rings of BTB06061 form hydrophobic interactions with the surrounding hydrophobic residues, including Val34, Leu37, Ala56 and Tyr79. As shown in the predicted model of HTS04781 with *H. pylori* UPPS, the sulfonamide group forms H-bonds with Gly16 and Arg26 and the N atom in the tetracyclic ring is hydrogen bound to the main chain of Met12. Extensive hydrophobic interactions were found between the tetracyclic ring with the surrounding residues including Met12, His30, Gly33 and Val34.

Surprisingly, BTB06061 showed 5-fold smaller IC_{50} (71 μM) against *E. coli* UPPS and HTS04781 almost did not inhibit *E. coli* UPPS, although two compounds inhibited *H. pylori* equally. From the modeling (not shown), the smaller entrance in *E. coli* UPPS compared to *H. Pylori* UPPS at the top of the tunnel due to the partial blockage by the amino acids such as Trp75 from the flexible loop might restrict, or at least partially limit the access of bulky compound HTS04781 that contains four rigid aromatic rings to the active site, thereby leading to the loss of inhibitory activity when competing with the substrate for binding.

4. DISCUSSION

In this paper we describe the crystal structures of UPPS from *H. pyroli*, a wide-spreading and life-threatening pathogen, and the first structure-derived inhibitors from computer virtual screening. Although a high-throughput screening has been performed for UPPS by a pharmaceutical company [24], none of the inhibitors have been reported. So far, a series of IPP analogues with a dicarboxylate moiety in place of the diphosphate were synthesized and the E-pentenylbutanedioic acid showed inhibition of UPPS with an IC_{50} of 135 μM [25]. Based on the known structure of UPPS (9), two carboxylate groups may coordinate with the catalytic Mg^{2+} ion which was bound with the pyrophosphate group of the substrates. Recently, we reported some bisphosphonates, which inhibited *trans*-type FPPs, which could also inhibit *cis*-type UPPS with sub-μM IC_{50} when containing suitable hydrophobic side-chains [26]. The crystal

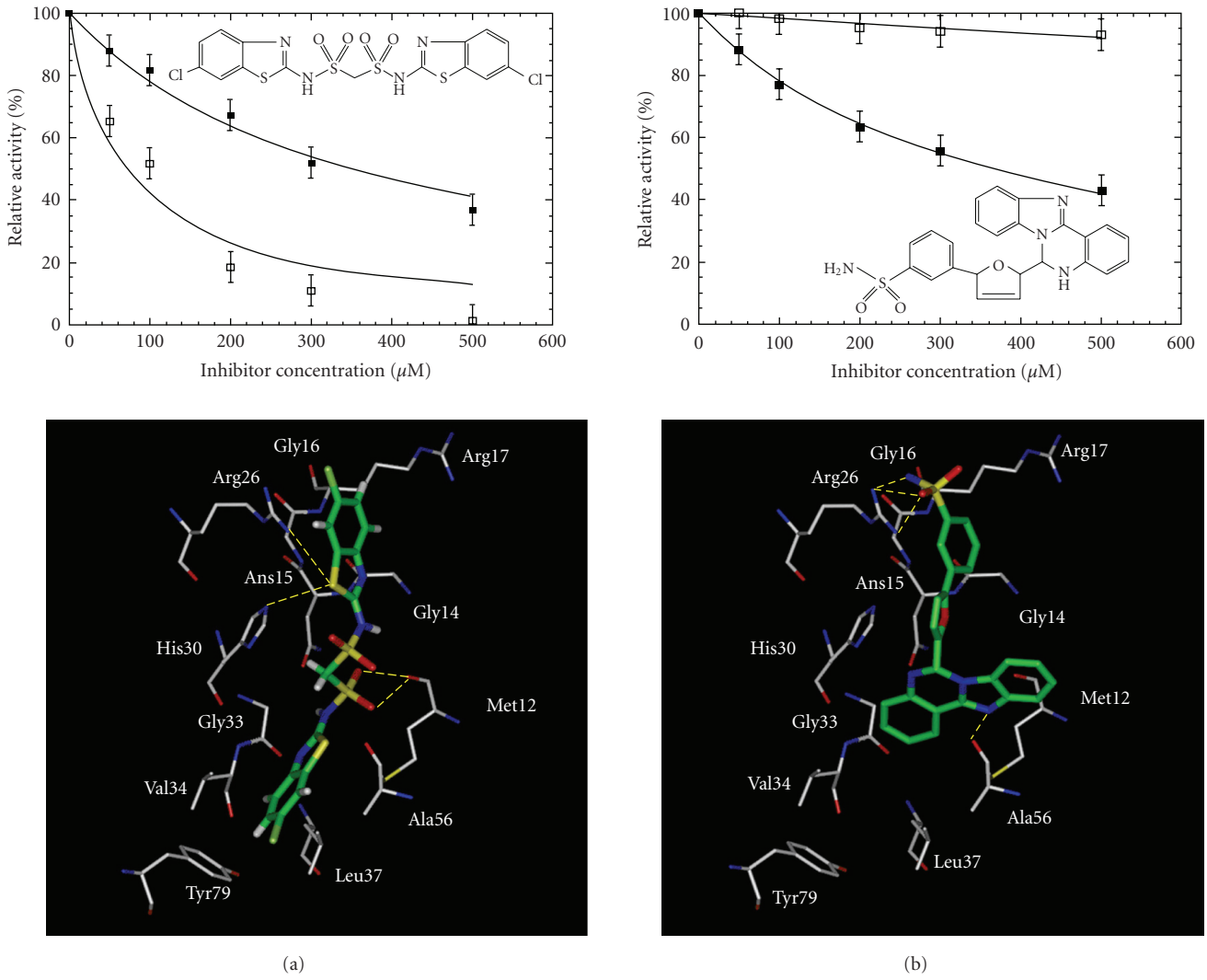

FIGURE 3: *Computer virtual screening of the H. pylori UPPS inhibitors.* Two compounds, BTB06061 shown in (a) and HTS04781 in (b), were identified from the computer fitting of the Maybridge compounds into the active site of *E. coli* and *H. pylori* UPPS. The data of enzyme activities in the presence of different concentrations of the inhibitors were used to determine the IC_{50} values of the inhibitors. The compounds displayed IC_{50} of 350 and 363 μM, respectively, in inhibiting *H. pylori* UPPS activity. However, the IC_{50} of BTB06061 became 71 μM in inhibiting *E. coli* UPPS and HTS04781 was almost inactive against the enzyme. The modeled structures of the inhibitor bound in the active site of *H. pylori* UPPS are shown at the bottom.

structures show that four molecules of inhibitors are bound in the active site and one of them occupies the FPP site with a phosphoate group chelating with the Mg^{2+}. Here, we report the first two novel inhibitors identified from a randomized compound library through virtual screening. These two inhibitors likely occupy the FPP site of *H. pylori* UPPS based on computer modeling. Two inhibitors displayed similar inhibition against *H. pylori* UPPS, but very different inhibition on *E. coli* UPPS. The one with bulky skeleton did not inhibit *E. coli* UPPS, likely owing to the partially blocked opening at the top of tunnel by the flexible loop in the *E. coli* UPPS active site. Our results shed light on the possibility of developing antibiotics specially targeting pathogenic *H. pylori* without killing the intestinal *E. coli*.

REFERENCES

[1] C. M. Allen, "Purification and characterization of undecaprenyl pyrophosphate synthetase," *Methods in Enzymology*, vol. 110, pp. 281–299, 1985.

[2] J. Robyt, *Essential of Carbohydrate Chemistry*, chapter 10, Springer, New York, NY, USA, 1998.

[3] K. Ogura and T. Koyama, "Enzymatic aspects of isoprenoid chain elongation," *Chemical Reviews*, vol. 98, no. 4, pp. 1263–1276, 1998.

[4] P.-H. Liang, T.-P. Ko, and A. H.-J. Wang, "Structure, mechanism and function of prenyltransferases," *European Journal of Biochemistry*, vol. 269, no. 14, pp. 3339–3354, 2002.

[5] A. Chen, P. A. Kroon, and C. D. Poulter, "Isoprenyl diphosphate synthases: protein sequence comparisons, phylogenetic

tree, and predictions of secondary structure," *Protein Science*, vol. 3, no. 4, pp. 600–607, 1994.

[6] N. Shimizu, T. Koyama, and K. Ogura, "Molecular cloning, expression, and purification of undecaprenyl diphosphate synthase. No sequence similarity between E- and Z-prenyl diphosphate synthases," *Journal of Biological Chemistry*, vol. 273, no. 31, pp. 19476–19481, 1998.

[7] C. M. Apfel, B. Takács, M. Fountoulakis, M. Stieger, and W. Keck, "Use of genomics to identify bacterial undecaprenyl pyrophosphate synthetase: cloning, expression, and characterization of the essential UPPS gene," *Journal of Bacteriology*, vol. 181, no. 2, pp. 483–492, 1999.

[8] H. Fujii, T. Koyama, and K. Ogura, "Efficient enzymatic hydrolysis of polyprenyl pyrophosphates," *Biochimica et Biophysica Acta*, vol. 712, no. 3, pp. 716–718, 1982.

[9] R.-T. Guo, T.-P. Ko, A. P.-C. Chen, C.-J. Kuo, A. H.-J. Wang, and P.-H. Liang, "Crystal structures of undecaprenyl pyrophosphate synthase in complex with magnesium, isopentenyl pyrophosphate, and farnesyl thiopyrophosphate: roles of the metal ion and conserved residues in catalysis," *Journal of Biological Chemistry*, vol. 280, no. 21, pp. 20762–20774, 2005.

[10] A. Nomura, G. N. Stemmermann, P. H. Chyou, G. J. Perez-Perez, and M. J. Blaser, "*Helicobacter pylori* infection and the risk for duodenal and gastric ulceration," *Annals of Internal Medicine*, vol. 120, pp. 977–981, 1994.

[11] F. Mauch, G. Bode, and P. Malfertheiner, "Identification and characterization of an ATPase system of *Helicobacter pylori* and the effect of proton pump inhibitors," *American Journal of Gastroenterology*, vol. 88, no. 10, pp. 1801–1802, 1993.

[12] P. Bytzer and C. O'Morain, "Treatment of *Helicobacter pylori*," *Helicobacter*, vol. 10, no. S1, pp. 40–46, 2005.

[13] S.-Y. Chang, T.-P. Ko, A. P.-C. Chen, A. H.-J. Wang, and P.-H. Liang, "Substrate binding mode and reaction mechanism of undecaprenyl pyrophosphate synthase deduced from crystallographic studies," *Protein Science*, vol. 13, no. 4, pp. 971–978, 2004.

[14] J.-J. Pan, L.-W. Yang, and P.-H. Liang, "Effect of site-directed mutagenesis of the conserved aspartate and glutamate on *E. coli* undecaprenyl pyrophosphate synthase catalysis," *Biochemistry*, vol. 39, no. 45, pp. 13856–13861, 2000.

[15] A. P.-C. Chen, S.-Y. Chang, Y.-C. Lin, et al., "Substrate and product specificities of cis-type undecaprenyl pyrophosphate synthase," *Biochemical Journal*, vol. 386, no. 1, pp. 169–176, 2005.

[16] Z. Otwinowski and W. Minor, "Processing of X-ray diffraction data collected in oscillation mode," *Methods in Enzymology*, vol. 276, pp. 307–326, 1997.

[17] A. T. Brunger, "Assessment of phase accuracy by cross validation: the free R value. Methods and applications," *Acta Crystallographica Section D*, vol. 49, no. 1, pp. 24–36, 1998.

[18] A. T. Brünger, P. D. Adams, G. M. Clore, et al., "Crystallography & NMR system: a new software suite for macromolecular structure determination," *Acta Crystallographica Section D*, vol. 54, no. 5, pp. 905–921, 1998.

[19] T. A. Jones, J. Y. Zou, S. W. Cowan, and M. Kjeldgaard, "Improved methods for building protein models in electron density maps and the location of errors in these models," *Acta Crystallographica Section A*, vol. 47, no. 2, pp. 110–119, 1991.

[20] P. J. Kraulis, "*MOLSCRIPT*: a program to produce both detailed and schematic plots of protein structures," *Journal of Applied Crystallography*, vol. 24, no. 5, pp. 947–950, 1991.

[21] E. A. Merritt and M. E. P. Murphy, "Raster3D version 2.0 A program for photorealistic molecular graphics," *Acta Crystallographica Section D*, vol. 50, no. 6, pp. 869–873, 1994.

[22] T.-P. Ko, Y.-K. Chen, H. Robinson, et al., "Mechanism of product chain length determination and the role of a flexible loop in *Escherichia coli* undecaprenyl-pyrophosphate synthase catalysis," *Journal of Biological Chemistry*, vol. 276, no. 50, pp. 47474–47482, 2001.

[23] S.-Y. Chang, T.-P. Ko, P.-H. Liang, and A. H.-J. Wang, "Catalytic mechanism revealed by the crystal structure of undecaprenyl pyrophosphate synthase in complex with sulfate, magnesium, and triton," *Journal of Biological Chemistry*, vol. 278, no. 31, pp. 29298–29307, 2003.

[24] H. Li, J. Huang, X. Jiang, M. Seefeld, M. McQueney, and R. Macarron, "The effect of triton concentration on the activity of undecaprenyl pyrophosphate synthase inhibitors," *Journal of Biomolecular Screening*, vol. 8, no. 6, pp. 712–715, 2003.

[25] A. A. Scholte, L. M. Eubanks, C. D. Poulter, and J. C. Vederas, "Synthesis and biological activity of isopentenyl diphosphate analogues," *Bioorganic and Medicinal Chemistry*, vol. 12, no. 4, pp. 763–770, 2004.

[26] R.-T. Guo, R. Cao, P.-H. Liang, et al., "Bisphosphonates target multiple sites in both cis- and trans- prenyltransferases," *Proceedings of the National Academy of Sciences of the United States of America*, vol. 104, no. 24, pp. 10022–10027, 2007.